Oncolytic Adenovirus ORCA-010 Activates Proinflammatory Myeloid Cells and Facilitates T Cell Recruitment and Activation by PD-1 Blockade in Melanoma

Milenova, Ioanna

2021-02-01

Milenova , I , Gonzalez , M L , Quixabeira , D C A , Santos , J M , Cervera-Carrascon , V , Dong , W , Hemminki , A , van Beusechem , V W , van de Ven , R & de Gruijl , T D 2021 , ' Oncolytic Adenovirus ORCA-010 Activates Proinflammatory Myeloid Cells and Facilitates T Cell Recruitment and Activation by PD-1 Blockade in Melanoma ' , Human Gene Therapy , vol. 32 , no. 3-4 , pp. 178-191 . https://doi.org/10.1089/hum.2020.277

http://hdl.handle.net/10138/328961
https://doi.org/10.1089/hum.2020.277

HGT

Oncolytic Adenovirus ORCA-010 Activates Proinflammatory Myeloid Cells and Facilitates T Cell Recruitment and Activation by PD-1 Blockade in Melanoma

Ioanna Milenova,[1,2] Marta Lopez Gonzalez,[1] Dafne C.A. Quixabeira,[3] Joao Manuel Santos,[3,4] Victor Cervera-Carrascon,[3] Wenliang Dong,[2] Akseli Hemminki,[3,4] Victor W. van Beusechem,[1,*] Rieneke van de Ven,[1,5] and Tanja D. de Gruijl[1]

Amsterdam UMC, Vrije Universiteit Amsterdam, Departments of [1]Medical Oncology and [5]Otolaryngology/Head-Neck Surgery, Cancer Center Amsterdam, Amsterdam Infection and Immunity Institute, Amsterdam, The Netherlands; [2]ORCA Therapeutics BV, 's-Hertogenbosch, The Netherlands; [3]Cancer Gene Therapy Group, Translational Immunology Research Program, Faculty of Medicine, University of Helsinki, Helsinki, Finland; [4]TILT Biotherapeutics Ltd., Helsinki, Finland.

Immune checkpoint inhibitors have advanced the treatment of melanoma. Nevertheless, a majority of patients are resistant, or develop resistance, to immune checkpoint blockade, which may be related to prevailing immune suppression by myeloid regulatory cells in the tumor microenvironment (TME). ORCA-010 is a novel oncolytic adenovirus that selectively replicates in, and lyses, cancer cells. We previously showed that ORCA-010 can activate melanoma-exposed conventional dendritic cells (cDCs). To study the effect of ORCA-010 on melanoma-conditioned macrophage development, we used an *in vitro* co-culture model of human monocytes with melanoma cell lines. We observed a selective survival and polarization of monocytes into M2-like macrophages ($CD14^+CD80^-CD163^+$) in co-cultures with cell lines that expressed macrophage colony-stimulating factor. Oncolysis of these melanoma cell lines, effected by ORCA-010, activated the resulting macrophages and converted them to a more proinflammatory state, evidenced by higher levels of PD-L1, CD80, and CD86 and an enhanced capacity to prime allogenic T cells and induce a type-1 T cell response. To assess the effect of ORCA-010 on myeloid subset distribution and activation *in vivo*, ORCA-010 was intratumorally injected and tested for T cell activation and recruitment in the human adenovirus nonpermissive B16-OVA mouse melanoma model. While systemic PD-1 blockade in this model in itself did not modulate myeloid or T cell subset distribution and activation, when it was preceded by i.t. injection of ORCA-010, this induced an increased rate and activation state of $CD8\alpha^+$ cDC1, both in the TME and in the spleen. Observed increased rates of activated $CD8^+$ T cells, expressing CD69 and PD-1, were related to both increased $CD8\alpha^+$ cDC1 rates and M1/M2 shifts in tumor and spleen. In conclusion, the myeloid modulatory properties of ORCA-010 in melanoma, resulting in recruitment and activation of T cells, could enhance the antitumor efficacy of PD-1 blockade.

Keywords: oncolytic adenovirus, macrophages, T cells, immune checkpoint inhibition, melanoma

INTRODUCTION

MELANOMA IS HIGHLY immunogenic, which explains its relative amenability to immunotherapy, but at the same time calls for powerful immune escape to allow melanoma tumors to grow and spread in the first place.[1,2] As a result, melanoma rapidly converts its tumor microenvironment (TME) into an immune suppressed state. This multifactorial suppression can also result in primary or acquired resistance to immune checkpoint blockade.[3,4] Tumor-associated M2-like macrophages (TAMs) are often the most abundant immune cell type in the tumor milieu and may play a dominant role in maintaining this immune suppressed and T cell-excluded microenvironment.[5–8]

Like all macrophages, TAMs found at the tumor site may develop either from recruited monocytes[9] or are tissue-resident macrophages and can acquire a phenotype positioned anywhere along the continuous spectrum from immune-suppressive M2 to T cell-stimulatory M1, depending on environmental cues.[10–13] *In vivo*, the release of

*Correspondence: Prof. Victor W. van Beusechem, Amsterdam UMC, Vrije Universiteit Amsterdam, Department of Medical Oncology, Cancer Center Amsterdam, Amsterdam Infection and Immunity Institute, De Boelelaan 1117, Amsterdam, The Netherlands. E-mail: vw.vanbeusechem@amsterdamumc.nl

DOI: 10.1089/hum.2020.277

macrophage-colony stimulating factor (M-CSF), TGF-β, interleukin (IL)-6, and/or IL-10 by melanoma converts monocytes into CD163$^+$ M2-like macrophages.[14–16] These cells themselves release soluble factors that dampen dendritic cell (DC) responses,[17] and attract T regulatory (Treg) cells.[18] Through the release of IL-10, they ultimately exclude CD8$^+$ T cells from their surroundings,[6,19] and support the tumor's progression.[20,21] On the opposite end of the continuous polarization spectrum, M1-like macrophages can release proinflammatory signals (IL-1β, IL-12, and tumor necrosis factor alpha [TNF-α]) and promote a CD8$^+$ T cell-mediated antitumor response through antigen presentation and co-stimulation through CD80 and CD86.[5,22,23]

Oncolytic adenoviruses (OAdVs) have entered clinical development and have shown favorable safety profiles; they are now being investigated as adjuvant therapies, alone or combined with chemotherapy or immunotherapy for melanoma, pancreatic cancer, and glioma (as recently reviewed[24]). Their role extends beyond simply inducing oncolysis. By inducing immunogenic cell death (ICD),[25,26] danger-associated molecular patterns (DAMPs) and (neo-)antigens are released into the TME.[27–29] The virus particles (VPs) themselves will also be taken up by antigen-presenting cells (APC), and serve as pathogen-associated molecular patterns (PAMPs), which are sensed by TLRs and induce activation of the APC,[30,31] although adenoviruses can also induce APC activation in a TLR-independent manner.[32] Together, these OAdV-induced triggers allow effective antitumor T cell responses to be launched.[28]

The effect of OAdV on macrophages has been studied in glioma mouse models,[33,34] but has not been characterized for melanoma as far as we are aware. Using *in vitro* culture models, we, in this study, show the effect of the OAdVs ORCA-010[35] on human monocyte-derived macrophages in the face of melanoma-induced suppression using an *in-vitro* co-culture model. We previously reported on the effects of ORCA-010 on the melanoma-conditioned differentiation of monocytes to dendritic cells (moDCs), in the presence of the moDC-inducing cytokines IL-4 and granulocyte-macrophage colony-stimulating factor (GM-CSF).[36] Here, we studied the effects of ORCA-010 on the unbiased melanoma-conditioned differentiation of monocytes. While the immature DCs and M2-like macrophages resulting from this melanoma conditioning are both immune-suppressive components of the TME, they are distinct cell populations with potentially different properties.

In addition, we have also studied the immune-modulating effects of ORCA-010 in the B16-OVA melanoma mouse model. Our data show the oncolysis-dependent activation of M2-like macrophages in human monocyte/melanoma co-cultures, as well as the direct proinflammatory effects of ORCA-010 *in vivo*. Based on these results, ORCA-010, with its potent oncolytic activity as well as local and systemic effects *in vivo*, could be an attractive candidate for overcoming resistance to immune checkpoint blockade in patients with melanoma.

MATERIALS AND METHODS

Cell lines

The human melanoma cell lines WM9, SK-MEL28, and MEL-57 were described previously.[36–40] Their identities were confirmed by short tandem repeat analysis (Eurofins, The Netherlands). The cell lines, including the B16-OVA murine melanoma cell line, were maintained as described previously,[36,41] and were tested for mycoplasma.

Viruses

ORCA-010 (Ad5-Δ24-T1-RGD)[35] is derived from human adenovirus serotype 5 and carries the following genetic modifications: the Δ24 mutation in the E1A region providing cancer cell-selective replication, the T1 mutation in the E3/19K gene that promotes oncolysis, and insertion of an Arg-Gly-Asp (RGD) motif in the fiber knob that enhances infection efficiency. The multiplicity of infection (MOI) used in cultures was chosen to achieve 60% lysed melanoma cells by day 6 of culture,[36] that is, MOI 25-IU/cell for SK-MEL28 and MEL57, and MOI 100-IU/cell for WM9. Replication-deficient adenovirus serotype 5 with an RGD motif and expressing luciferase under a CMV promoter (Ad5-Luc-RGD)[42] was used at MOI 100-IU/cell. The OAdVs ONYX-015[43] and Ad5-Δ24-RGD[44] are conditionally replicative, and carry an E1B-55K deletion mutation, or an E1A modification and RGD insertion, respectively.

Isolation of peripheral blood lymphocytes and monocytes

Peripheral blood mononuclear cells (PBMCs) were isolated from buffy coats from consenting healthy donors (Sanquin Blood Supply Services, The Netherlands) and from these, CD14$^+$ monocytes were isolated by magnetic bead separation, as previously described.[36,45]

Monocyte-derived macrophage polarization

Control macrophages (*i.e.*, generated without melanoma cell lines) were derived by culturing CD14$^+$ monocytes in complete RPMI medium (RPMI-1640 medium+Glutamine & L-HEPES; ThermoFisher, Waltham, MA), with fetal calf serum (10% FSC HyClone; GE, Boston, MA), penicillin-streptomycin-glutamine (1% P/S/G; ThermoFisher), and beta-2-mercaptoethanol (5.5 mM; ThermoFisher) supplemented with 0.1 μg/mL M-CSF (ImmunoTools, Germany), or GM-CSF (1,000 IU/mL; ImmunoTools), to develop into resting M2-like and M1-like macrophages, respectively.[46] To activate the M2-like macrophages, after 7 days of culture,[47] a cocktail of recombinant human IL-4 (0.02 μg/mL rhIL-4; R&D Systems,

Minneapolis, MN) and rhIL-10 (0.01 μg/mL; eBioscience, ThermoFisher) was added. M1-like macrophages were activated with lipopolysaccharide (0.1 μg/mL LPS; Sigma Aldrich, St. Louis, MO) and interferon gamma (1,000 IU/mL IFNγ; R&D Systems) on day 7. Supernatants were collected after 24 h (day 8), and phenotyping was done by flow cytometry.

Melanoma cell lines were plated in 500 μL complete RPMI medium. ORCA-010 was added 24 h later, 4 h before the addition of 2×10e5 $CD14^+$ monocytes, in a 1:10 melanoma-to-monocyte ratio. ORCA-010 was added to the melanoma cells 4 h before the monocytes were added, to maximize virus uptake by the tumor cells. One hundred microliters of supernatant was collected from the culture on days 3, 7, and 8, and replaced by the same amount of complete RPMI medium. Flow cytometry was performed on day 8 (see Fig. 1A for timeline).

Alternatively, supernatants were collected from the melanoma cell lines after 48 h of culture and run through a 0.22 μm Millex-GV Syringe Filter Unit (Merck KGaA, Germany). The $CD14^+$ monocytes were plated with 60% tumor-derived supernatant (TDSN) and 40% complete RPMI medium, and cultured for 8 days (Fig. 1B). Viability was determined by flow cytometry with 7-amino-actinomycin D (7-AAD) cell dye (Sigma, Ronkonkoma, NY), and the cells were phenotyped or assessed for their T cell priming capability as described below.

Mixed leukocyte reaction

On day 8 of the co-culture, the cells were harvested, and the macrophages were separated from the tumor cells by CD45 MACS according to the manufacturer's protocol (Miltenyi-Biotec, Germany). Purity (>90%) was checked by flow cytometry. Peripheral blood lymphocytes (PBLs) from healthy donor PBMCs depleted from monocytes by CD14 MACS were labeled with intracellular fluorescent dye 5,6-carboxyfluorescein diacetate succinimidyl ester (3 μM CFSE; Sigma Aldrich). CFSE-labeled PBLs (10e5 cells per well) were cultured in a 96-well round-bottom plate (Greiner Bio-One, Germany) in triplicate in a 10:1 ratio with macrophages (10,000 cells/well), in 200 μL complete RPMI medium. Positive control for T cell stimulation was CFSE-labeled PBLs stimulated at the start of culture with phytohemagglutinin (5 μg/mL PHA; Oxoid). The mixed leukocyte reaction (MLR) was cultured for 6 days, at which point, supernatants were collected and flow cytometry was performed to assess proliferation.

Flow cytometry

Macrophage cultures were washed and fixed with phosphate-buffered saline (PBS; Fresenius Kabi, The Netherlands) supplemented with bovine serum albumin (0.5 g BSA; ThermoFisher) and sodium azide (0.1%; Sigma Aldrich), and stained with the following anti-human antibodies: CD45 AF700 (clone HI30; Biolegend), CD14 FITC (clone MΦP9; BD Biosciences, San Diego, CA), CD163 PE (clone GHI/61; Sony Biotechnology, San Jose, CA), CD80 BV421 (clone 2D10; Biolegend), CD86 PCP-Cy5.5 (clone 2331 [FUN-1]; BD Pharmingen), PD-L1 APC (clone MIH1; eBioscience), and HLA-DR FITC (clone L243; BD Pharmingen).

T cells and macrophages from an MLR culture were fixed and stained with the following antibodies: CD14 PE-CF594 (clone Mφ-P9; BD Biosciences), CD3 BV421 (clone SK7; BD Horizon), CD4 AF700 (clone RPA-T4; BD Pharmingen), and CD8 APC (clone SK-1; BD Biosciences). Viability was determined with 7-AAD cell viability dye (Sigma). The samples were acquired on a Fortessa X20 flow cytometer (Becton-Dickinson, Franklin Lakes, NJ), and analyzed with Kaluza Analysis software 1.3 (Beckman Coulter Life Sciences, Indianapolis, IN).

For phenotypic analysis of the mouse immune populations (described below), tumors and spleens harvested on day 10 were processed into single-cell suspension and fluorescently labeled with the anti-mouse antibodies listed in Supplementary Table S1. The phenotypic definitions of the myeloid populations are listed in Supplementary Table S2, as described previously.[48–55] Samples were acquired on the Sony SH800 cytometer (Sony Biotechnology), and analyzed with Kaluza analysis software 1.3 (Beckman Coulter Life Sciences).

To determine IFNγ secretion by ovalbumin (OVA)-reactive T cells, mouse splenocytes were thawed, passed through a 100 μm cell strainer (BD), and restimulated *in vitro* for 4–5 h with 1 μg/mL OVA-derived SIINFEKL peptide[56] (a kind gift of Prof. Yvette van Kooyk,

Figure 1. Suppression by melanoma cell lines, and oncolysis by ORCA-010. The phenotype of monocyte-derived macrophages was determined by culturing $CD14^+$ monocytes (isolated from healthy donor PBMCs), with melanoma cell lines M57, WM9, and SK-MEL28 *in vitro*. **(A)** The co-culture and **(B)** TDSN culture timelines, as detailed in the Materials and Methods. **(C)** Representative *dot plots* of CD45 and CD14 (*top row*), and the scatter properties of the $CD14^+CD45^+$ population (FSC and SSC; *bottom row*) for each co-culture and activated M2-like and M1-like macrophage controls. **(D)** Bar graphs with the percentage total $CD45^+$ cells (*gray bars*) in co-cultures with SK-MEL28, M57, and WM9, and the percentage of live $CD45^+$ cells upon culture in supernatant derived from SK-MEL28, M57, and WM9 (TDSN; *white bars*). **(E)** Representative histogram plots for the expression of CD163, PD-L1, CD80, CD86, and CD14 on macrophages in a co-culture with M57, WM9, or SK-MEL28, compared to activated M2-like and M1-like control macrophages. The FMO control for each marker is delineated by the marker in the histogram. The MFI of every marker is listed. **(F)** Incucyte live-cell images of $CD14^+$ monocytes cultured with M-CSF (*top*) or GM-CSF (*bottom*), compared to co-cultures with M57, WM9, or SK-MEL28 without ORCA-010 (*medium*; *top row*) or with ORCA-010 (*bottom row*). Magnification is 20×. Distinct macrophage morphology (*black arrow*), and cell debris (*white arrow*) are shown on the images. Data shown are mean ± SEM for $n=3$. Significant p-values by paired t-test are shown. FMO, fluorescence minus one; GM-CSF, granulocyte-macrophage colony-stimulating factor; M-CSF, macrophage colony-stimulating factor; MFI, mean fluorescent intensity; PBMCs, peripheral blood mononuclear cells; SEM, standard error of mean; TDSN, tumor-derived supernatant.

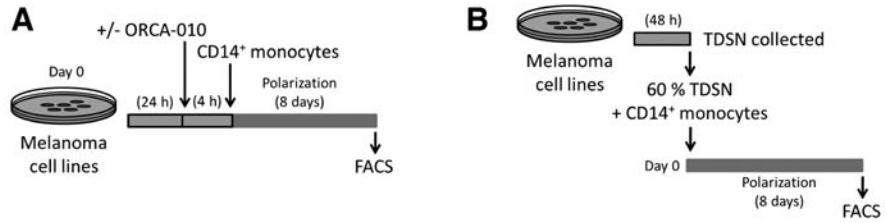

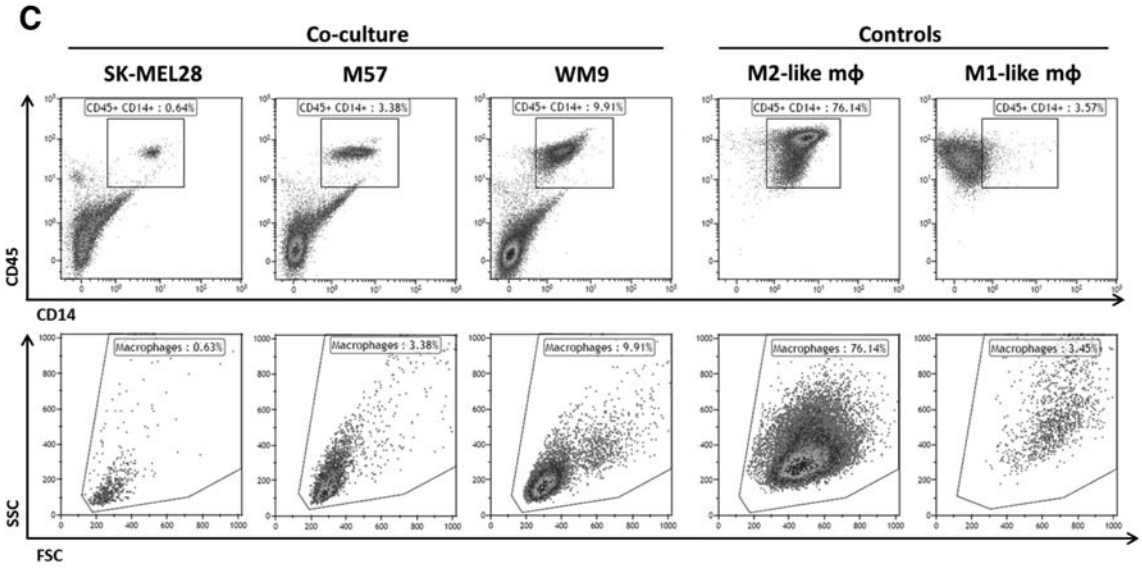

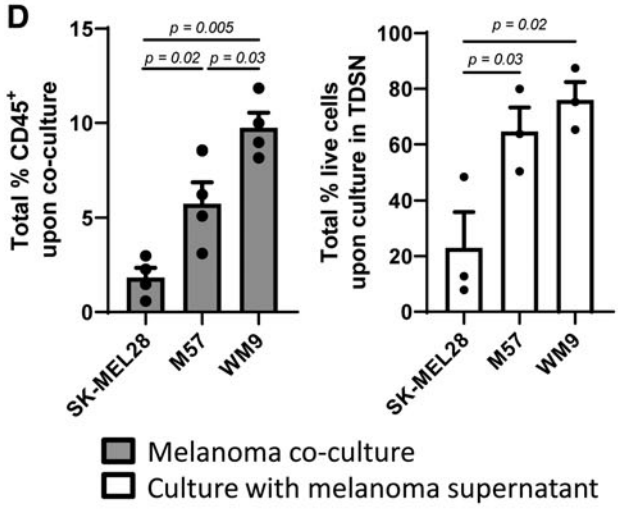

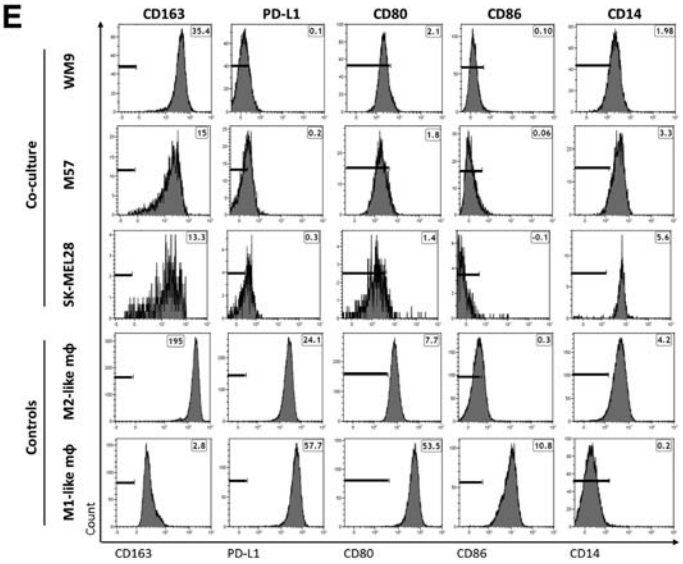

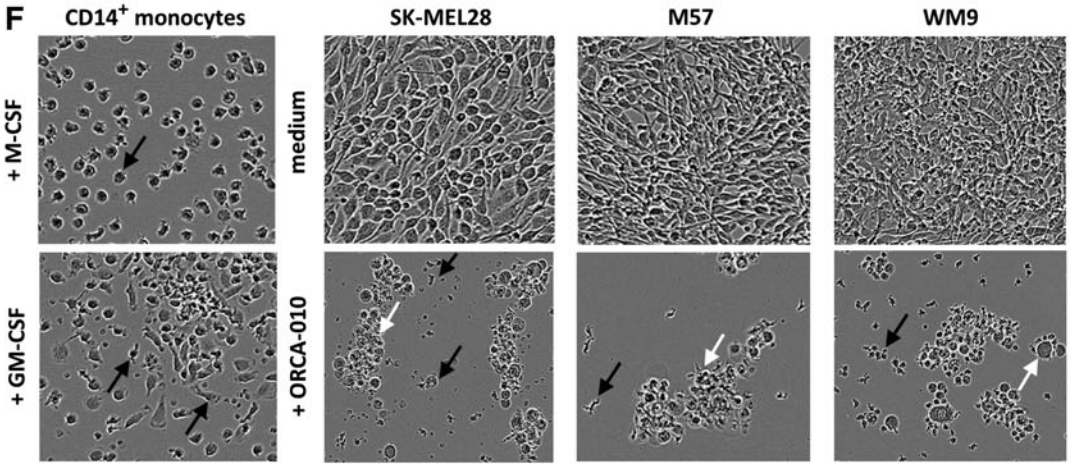

Amsterdam UMC, The Netherlands) and 1:500 GolgiPlug™ protein transport inhibitor containing Brefeldin A (BD Biosciences). After washing, cells were stained for 20 min in 1:5,000 fixable viability dye eFluor™ 506 (eBioscience, San Diego, CA) diluted in PBS to detect dead cells, followed by an FcγII- and FcγIII-receptor blocking step using the 2.4G2 antibody (BD Biosciences). Following washing, the cells were stained with membrane anti-mouse antibodies (CD3 and CD8, see Supplementary Table S1). IFNγ FITC (Supplementary Table S1) was intracellularly stained in cells permeabilized with the eBioscience™ FoxP3/Transcription Factor Staining Buffer Set (ThermoFisher). Samples were acquired on the Fortessa X20 flow cytometer (Becton-Dickinson) and analyzed on Kaluza Analysis Software v1.3 (Beckman Coulter, Miami, FL).

Cytokine profiling

Supernatants collected from the *in vitro* cultures and MLR were analyzed for IL-6, IL-8, IL-10, IL-1b, TNF-α, and IL-12p70 using the human inflammatory cytometric bead array (CBA) kit (BD Biosciences), and for IL-2, IL-4, IL-6, IL-10, IFN-y, TNF-α, and IL17A using the human Th1/Th2/Th17 CBA kit (BD Biosciences), respectively. The samples were acquired on a Fortessa X20 flow cytometer (Becton-Dickinson), and analyzed with FCAP Array 3 software (BD Biosciences).

In vivo experiment design and treatments

Four- to 6-week-old C57BL/6 JOlaHsd immunecompetent female mice (Envigo, Indianapolis, IN) were quarantined for 1 week, and housed in a Biosafety level II facility. All animal protocols were reviewed and approved by the experimental animal committee of the University of Helsinki (Finland) and the Provincial Government of Southern Finland. Mice were engrafted subcutaneously with 0.25×10^6 B16-OVA cells in 100 μL RPMI-1640 medium in the left flank. The tumor growth was monitored daily until day 11 when tumors reached 3–4 mm in length. The mice were randomly distributed into four groups ($n = 4$ per group), namely PBS, ORCA-010, anti-PD-1, and ORCA-010 plus anti-PD-1, and treatments were initiated (day 0).

Tumors received 1×10^9 ORCA-010 VP intratumorally (i.t.) in saline mixed with filter-sterilized dimethyl sulfoxide (12% v/v DMSO; Sigma) on days 0, 1, 3, 6, and 9. Groups treated with anti-mouse PD-1 InVivoMAb (7.23 mg/mL, clone RMPI-14; BioXCell, Lebanon, NH) were injected into the peritoneum (i.p.) on days 3, 6, and 9. The vehicle control group received saline with filter-sterilized DMSO i.t. and saline i.p. following the same schedule as the groups receiving therapy. A prime-boost treatment strategy was followed as described previously.[41] Health was monitored daily, and tumor volume was measured daily. Mice were anaesthetized with 2% isoflurane (Piramal Healthcare) for all treatments and tumor measurements. Tumor volume was calculated as $0.5 \times (\text{shortest diameter})^2 \times \text{longest diameter}$. To characterize the effect of ORCA-010 and PD-1 blockade on the immune response at the same time point, all mice were sacrificed 10 days after treatments began, and the tumor and spleen were collected, dissociated into single-cell suspension, and frozen at −80°C until further analysis. Euthanasia was performed before the experimental endpoint if mice had an ulcer (open wound) at the injection site, or if the tumor volume exceeded 18 mm. In the vehicle control group, one mouse was found dead in the cage on day 10, while in the combination group, one mouse was sacrificed on day 9 due to an ulcer on the tumor.

Transcriptional analysis

CD163 (gene ID: 9332) and *CSF-1* (M-CSF; gene ID: 1435) transcript levels from the publicly available dataset ''Tumor Skin Cutaneous Melanoma TCGA'' (TCGA-470-rsem—tcgars; source ID: SKCM) were correlated using R2 software (R2: Genomics Analysis and Visualization Platform). This dataset was selected because of the high sample number. No further distinctions based on disease progression or metastasis were made.

Statistical analysis

All data were tested for significance with GraphPad Prism version 8 (San Diego, CA). Student's *t*-test was used for significance testing of *in vitro* experiments. One-way analysis of variance with Holm-Sidak's multiple comparisons test was used to determine significance of the *in vivo* mouse experiments. *p*-Values <0.05 were considered significant and are indicated in the graphs.

RESULTS

Melanoma-mediated survival and polarization of M2-like macrophages

The effect of human melanoma cell lines on human $CD14^+$ monocytes was evaluated by both co-cultures with the melanoma cells (Fig. 1A) or culture with cell line-derived supernatants TDSN (Fig. 1B). In co-cultures and cultures with TDSN, the M57 and WM9 cell lines supported survival of $CD45^+CD14^+$ monocytes (which acquired macrophage-like scatter properties), whereas SK-MEL28 did not (Fig. 1C, D), demonstrating the presence of soluble melanoma-derived factors able to support monocyte survival. In co-cultures, the monocytes skewed to an M2-like phenotype ($CD14^+CD163^+$) with absent or low expression levels of the B7-family members CD80, CD86, and PD-L1 (Fig. 1E). With a round appearance, morphologically, they resembled more M2- than M1-like macrophages (Fig. 1F).

Of note, M-CSF- and GM-CSF-induced M2 and M1 monocyte-derived macrophages, activated by polarizing cytokine cocktails, were included in phenotypic and morphological assessments to denote two ends of the

macrophage polarization spectrum. The onco-mutational status of the tested cell lines and their secretion levels of growth factors and cytokines were previously reported by us.[36] The three tested cell lines, in varying degrees, produced low levels of IL-10 and IL-6, but WM9 and M57 uniquely produced M-CSF, a potent growth and survival factor for M2-like macrophages.[11,16] The importance of M-CSF in this regard was confirmed by a strong correlation between the M2-related *CD163* and *M-CSF* transcript levels in a TCGA data set of $n=470$ melanoma samples (Supplementary Fig. S1). WM9, because of its metastatic origin, its BRAF and PTEN mutation status,[36] both related to immune suppression and T cell exclusion,[51,57] and its ability to secrete M-CSF, was chosen as the model cell line to further study the effects of ORCA-010-induced oncolysis in co-cultures with monocytes *in vitro*.

Oncolysis of melanoma cells by ORCA-010 activates macrophages, resulting in their increased capacity to prime type-1 T cells

Infection of WM9 melanoma cells with ORCA-010 over the course of 4 h at an MOI of 100, before addition of monocytes for a subsequent 8-day co-culture (Fig. 1A), did not prevent expression of the M2-associated markers CD14 and CD163 on the melanoma-conditioned macrophages (Fig. 2A, B), but it did lead to their increased forward and side scatter properties consistent with a more M1-like morphology (Fig. 2A). This was confirmed by significant upregulation of CD80, CD86, and PD-L1, similar to the expression profile of M1-macrophages (Fig. 2B, C). Of note, polychromatic staining showed that although CD80, CD86, and PD-L1 were upregulated by ORCA-010, CD163 was not downregulated on the same $CD14^+$ cells: as such, macrophage activation was observed, rather than classic M2-to-M1 skewing.

Similar observations for CD86 were made for the M57, and to a lesser extent, SK-MEL-28 cell lines (data not shown). A comparison with nonreplicative adenovirus (Ad5-Luc-RGD) showed this activation to be specific to the OAdV ORCA-010 (Fig. 2D), and was therefore, in this model, more likely related to DAMPs, released upon ORCA-010-induced oncolysis (Fig. 1F), than to adenovirus-derived PAMPs. Indeed, Ad5-Δ24-RGD, which, similar to ORCA-010, was able to induce oncolysis in WM9 melanoma cells, also induced upregulation of the B7 family members CD80, CD86, and PD-L1 on monocyte-derived macrophages, whereas ONYX-015, an adenovirus with attenuated oncolytic potential in comparison to Δ24-type viruses, which did not induce detectable oncolysis in WM9 melanoma cells, did not (Supplementary Fig. S2). Importantly, macrophages isolated from ORCA-010-infected WM9 co-cultures displayed a significantly improved ability over macrophages differentiated in untreated WM9 co-cultures to prime and activate both $CD4^+$ and $CD8^+$ T cells in a 6-day allogeneic MLR (Fig. 3A–C). These primed T cells generally secreted higher levels of the type-1 cytokines IFNγ, IL-2, and TNF-α (Fig. 3D). Significantly higher IFNγ:IL-10 and IFNγ:IL-4 (ns) ratios indeed confirmed type-1 effector T cell skewing.

Intratumoral delivery of ORCA-010 combined with systemic PD-1 blockade promotes a systemic inflammatory response and increased $CD8^+$ T cell infiltration

To assess the effects of ORCA-010 on the recruitment and activation of myeloid subsets and T cells *in vivo*, B16-OVA bearing syngeneic BL6 mice were treated intratumorally with ORCA-010, followed by systemic anti-PD-1 administration[41] (Fig. 4A). At the time of sacrifice (day 10), the mean tumor volume was the same for all groups (Fig. 4B), consistent with the fact that murine tumors are not permissive to OAdV replication and therefore will not undergo oncolysis. Myeloid and T cell subsets were assessed by flow cytometry in both tumors and spleens.

In the tumor, no differences in frequencies of myeloid-derived suppressor cells (MDSC, data not shown) or TAMs were observed, nor any treatment-related shifts in M1-M2 phenotypes; rather, a significant increase was observed in $CD8\alpha^+$ conventional dendritic cell 1 (cDC1) upon combined ORCA-010 administration and PD-1 blockade (Fig. 4C). Combined ORCA-010 and PD-1 treatment also increased rates of tumor-infiltrating $CD8^+$ T cells in an activated state as evidenced by their increased CD69 expression (Fig. 4D). Numbers of $CD8^+$-infiltrating T cells were strongly correlated to tumor-associated $CD8\alpha^+$ cDC1, both of which were recruited upon i.t. ORCA-010 delivery (Fig. 4E, left panel). PD-1 expression levels on

Figure 2. Oncolysis by ORCA-010 induces activated macrophages in a co-culture with WM9 melanoma cell line. After 8 days of co-culture with the WM9 melanoma cell line, the phenotype of the $CD45^+$ monocyte population was determined by flow cytometry. **(A)** Representative *dot plots* of the $CD45^+CD14^+$ population (*top row*) and the scatter properties within that gate (FSC, SSC; *bottom row*) for WM9 co-culture without ("medium") or with ORCA-010 ("+ORCA-010"), compared to activated M2-like and M1-like control macrophages. **(B)** Representative *dot plots* for the co-expression of markers on $CD45^+$ macrophages in WM9 co-culture without ("medium"; *left panel*) or with ORCA-010 (*right panel*). Activated M2-like and M1-like macrophages are included as controls. Gates were set on FMO controls. **(C)** The corresponding bar graphs of the *dot plots* in **(B)**, with the percentage of marker co-expression on macrophages from WM9 co-culture without "medium" (*light gray*) or with ORCA-010 (*dark gray*) ($n=5$, mean ± SEM). **(D)** Macrophages from a WM9 co-culture infected with a replication-deficient adenovirus vector (Ad5-Luc-RGD) or with ORCA-010 were phenotyped on day 8 of co-culture by flow cytometry. The MFI of macrophage-associated markers HLA-DR, CD80, CD86, and PD-L1 are shown for WM9 co-culture with Ad5-Luc-RGD (*light gray*) or ORCA-010 (*dark gray*), relative to the expression on macrophages from an uninfected WM9 co-culture (shown by a *solid line* at $y=1$). Data are mean ± SEM for $n=3$. Significant *p*-values of paired *t*-test are shown.

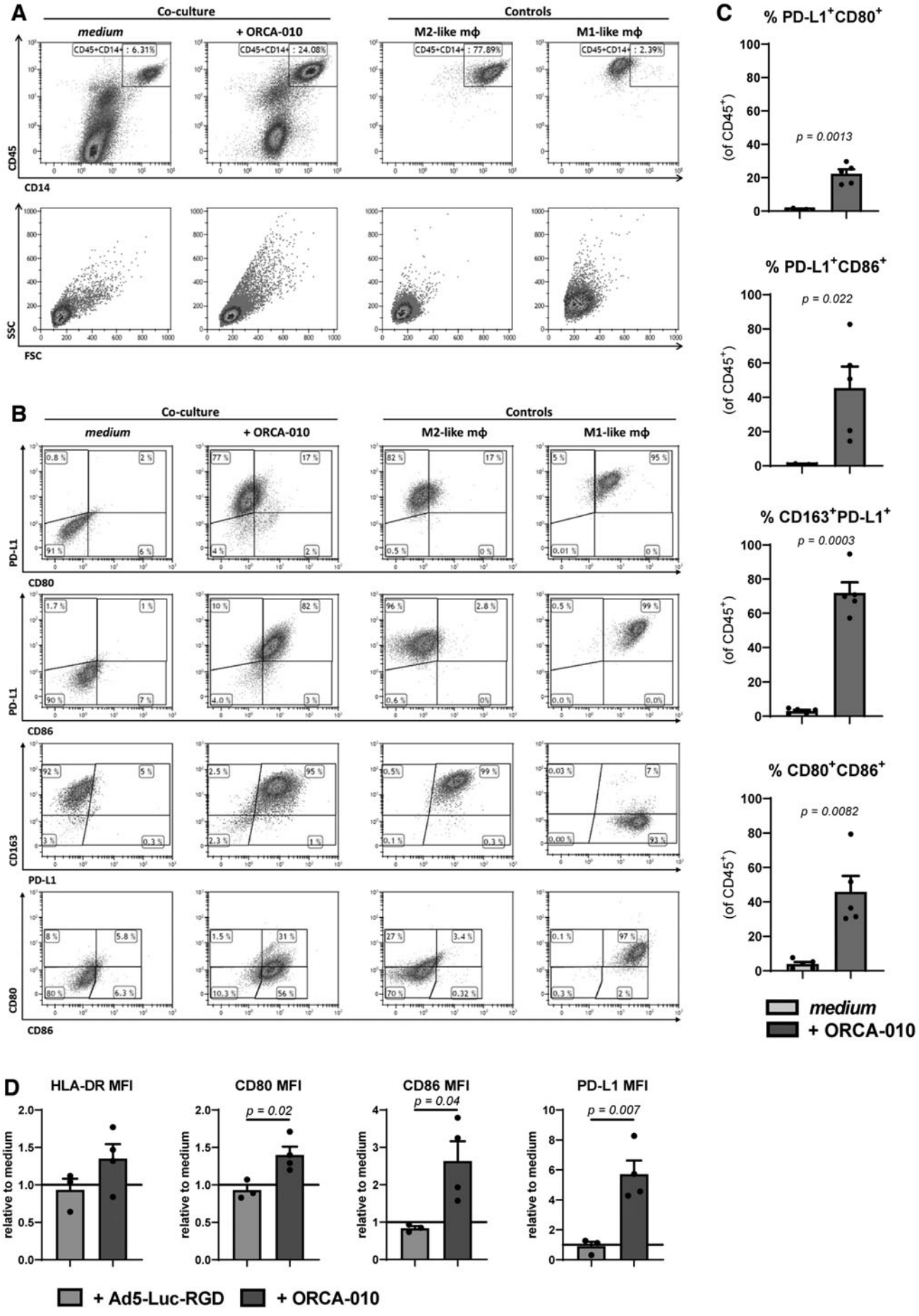

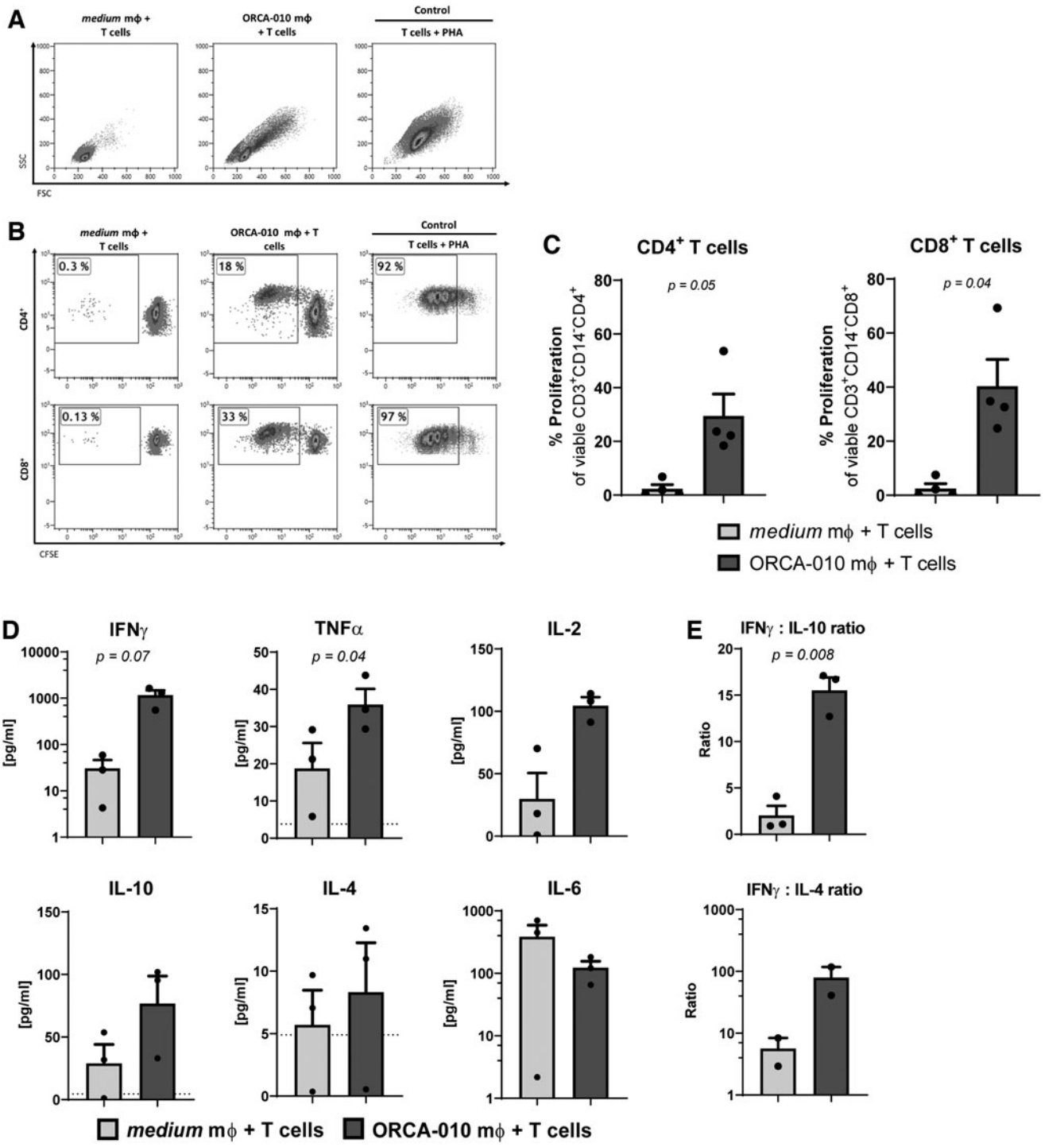

Figure 3. Activated macrophages from a WM9 co-culture with ORCA-010 can expand T cells in an allogeneic MLR and induce the secretion of Th1 cytokines. After 8 days, macrophages were sorted from co-cultures with melanoma cells based on CD45, and were subsequently cultured in a 1:10 target-to-effector ratio with CFSE-labeled, non-HLA-matched T cells for 6 days, upon which T cell proliferation was assessed by flow cytometry. Cytokines were quantified in 6-day MLR supernatants. **(A)** The scatter properties (FSC and SSC) of lymphocytes cultured with macrophages from WM9 co-culture alone ("medium"), or with ORCA-010, compared to control T cells cultured with PHA, gated on viable $CD3^+$ cells. **(B)** For each MLR condition, the *dot plots* illustrate the proliferation (CFSE signal) of $CD4^+$ (*top row*) and $CD8^+$ (*bottom row*) T cells. **(C)** The percentage proliferated ($CFSE^{lo}$) CD4 and CD8 T cells ($n=4$; mean ± SEM). **(D)** Cytokine concentrations (pg/mL) of IFNγ, TNF-α, IL-2, IL-10, IL-4, and IL-6 and **(E)** IFNγ:IL-10 and IFNγ:IL-4 ratios on day 6 of MLR ($n=3$; mean ± SEM). The *dotted line* in bar graphs shows the lower limit of detection. Statistical significance (paired *t*-test) is indicated as *p*-values. IFNγ, interferon gamma; IL, interleukin; MLR, mixed leukocyte reaction; PHA, phytohemagglutinin; TNF-α, tumor necrosis factor alpha.

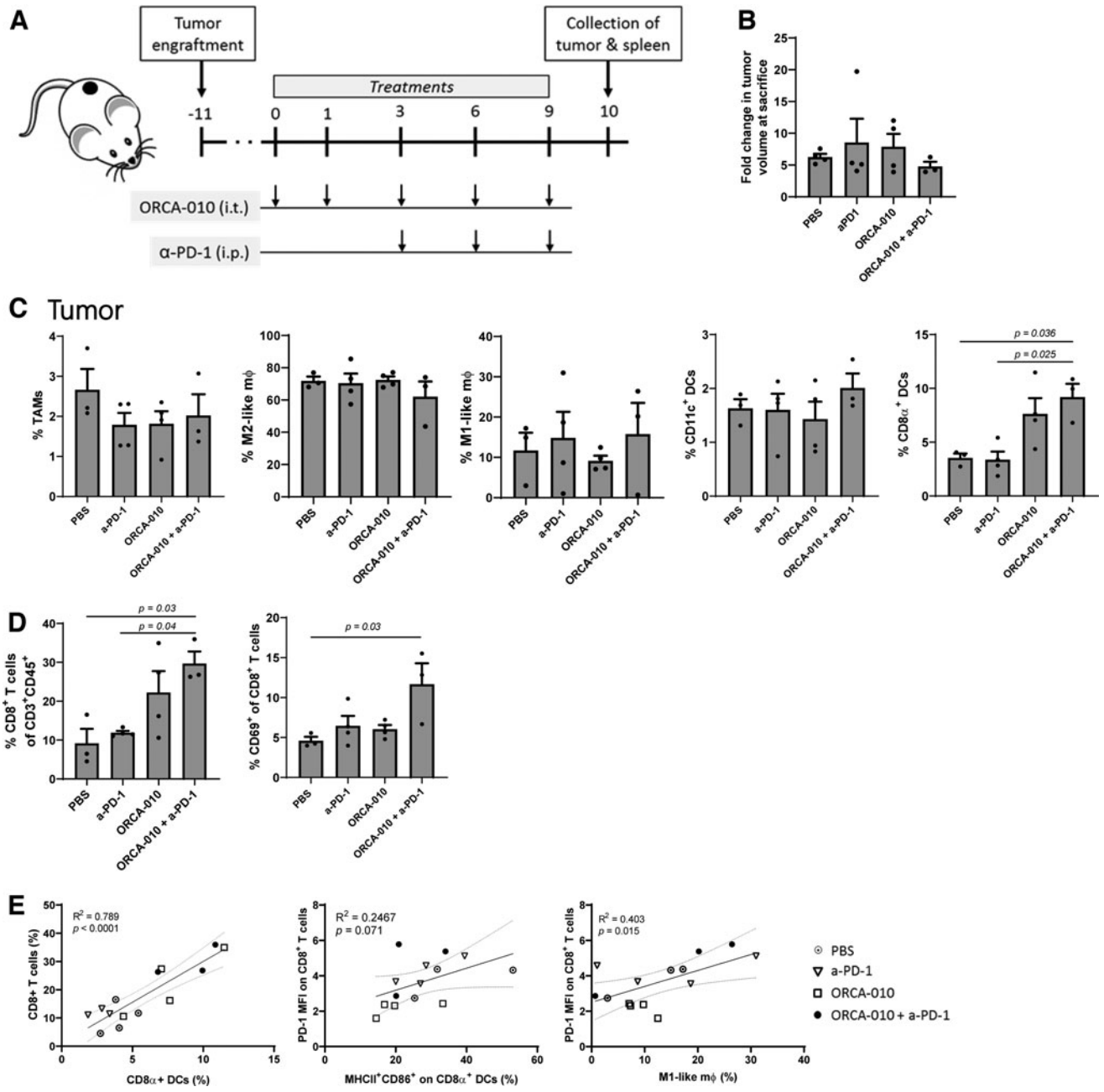

Figure 4. ORCA-010 and anti-PD-1 combination therapy induces T cell infiltration and activation in B16-OVA melanoma tumors. **(A)** The treatment schedule in C57BL/6 mice. PBS and ORCA-010 were injected intratumorally (i.t.), and anti-PD-1 was administered systemically (i.p.) ($n=4$ per group). **(B)** The fold change in tumor volume (mm^3) on the day of sacrifice. **(C)** The percentage of TAMs, M2-like and M1-like macrophages, cDCs, $CD8\alpha^+$ cDCs, and **(D)** $CD8^+$ T cells and $CD69^+CD8^+$ T cells are shown. Significance by one-way ANOVA is indicated as p-values for $n=3$–4 mice per group. Note: In the vehicle control group, one mouse was found dead in the cage on day 10, while in the combination group, one mouse was sacrificed on day 9 due to an ulcer on the tumor. **(E)** Correlation between $CD8^+$ T cells and $CD8\alpha^+$ DCs (*left panel*), PD-1 MFI on $CD8^+$ T cells and activated $CD8\alpha^+$ DCs (*middle panel*), and PD-1 MFI on $CD8^+$ T cells and M1-like macrophages (*right panel*) in the tumor. Linear regression was used to calculate the correlation coefficient (R^2) and p-value. ANOVA, analysis of variance; cDC, conventional dendritic cell; OVA, ovalbumin; PBS, phosphate-buffered saline; TAM, tumor-associated M2-like macrophage.

tumor-infiltrating $CD8^+$ T cells, a sign of tumor specificity,[58,59] were related to both activation of $CD8\alpha^+$ cDC1 and M1-like macrophage content (Fig. 4E, right panels).

In the spleen, M2-like macrophages decreased, and $CD11c^+$ cDC and $CD8\alpha^+$ cDC1 increased in response to ORCA-010 and anti-PD-1 combination treatment (Fig. 5A). This was accompanied by increases in both $CD8^+$ and $CD4^+$ T cells in a combination treatment-induced activation state, as evidenced by increases in PD-1 expression rates (Fig. 5B). Upon *in vitro* restimulation of splenocytes with the immunodominant OVA-derived epitope SIINFEKL, low-frequency OVA-reactive $CD8^+$ T cells producing IFNγ were measurable by day 10 after intratumoral delivery, confirming the priming of tumor-

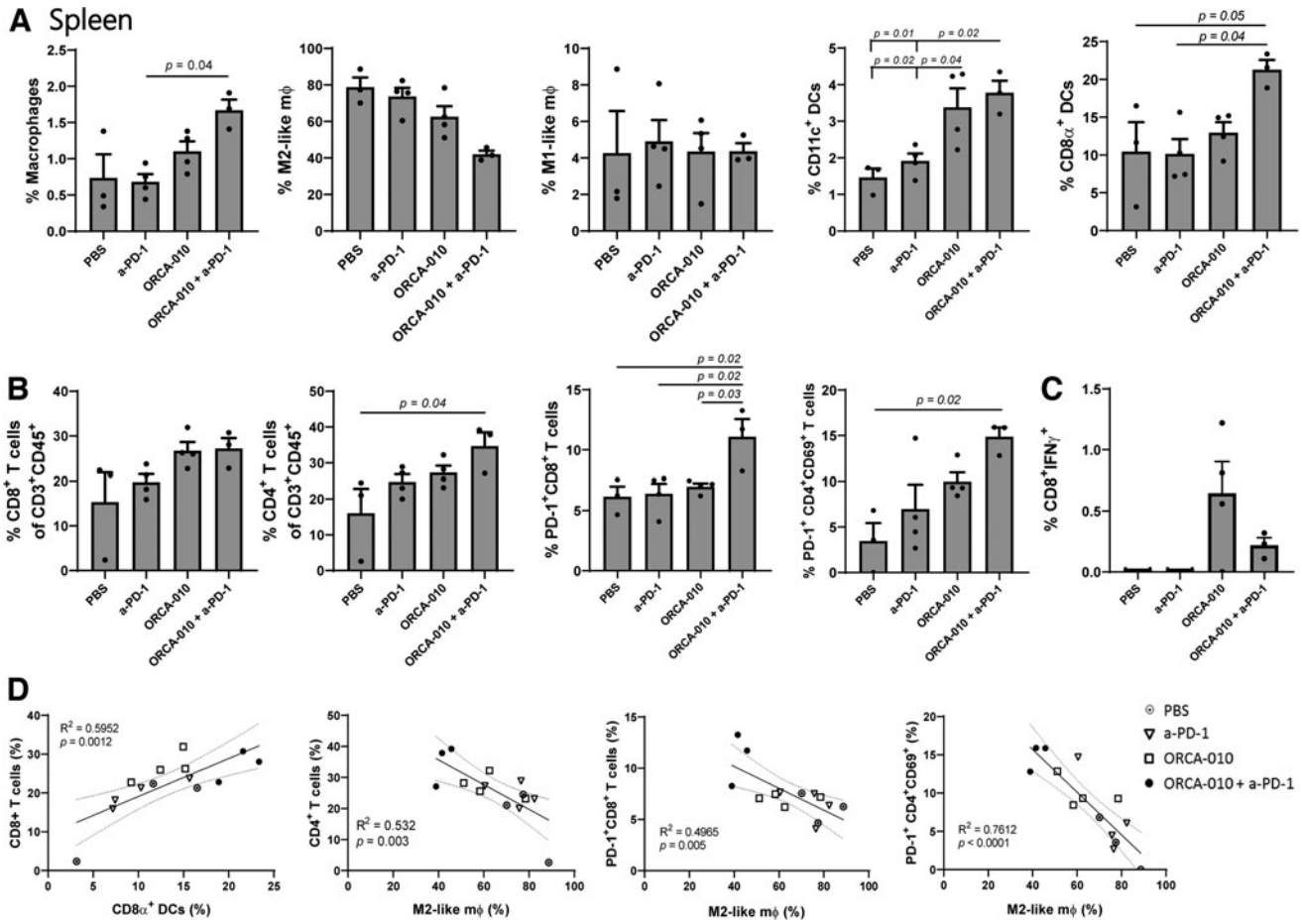

Figure 5. Rates and activation state of immune cell subsets in the spleen of ORCA-010 and anti-PD-1-treated B16-OVA tumor-bearing mice. Phenotypic analysis of cells in the spleen of mice, 10 days after the start of treatment. **(A)** Percentage of macrophages, M2-like and M1-like macrophages, CD11c$^+$ cDCs, CD8α^+ cDCs, and **(B)** CD8$^+$ T cells, CD4$^+$ T cells, PD-1$^+$CD8$^+$, and PD-1$^+$CD4$^+$CD69$^+$ T cells. **(C)** The percentage of CD8$^+$IFNγ^+ T cells following *in vitro* restimulation of splenocytes with OVA-specific SIINFEKL peptide. **(D)** Correlation, from *left*-to-*right*, between CD8$^+$ T cells and CD8α^+ cDCs, and CD4$^+$, PD-1$^+$CD8$^+$, and PD-1$^+$CD4$^+$CD69$^+$ T cells with M2-like macrophages, respectively. Note: In the vehicle control group, one mouse was found dead in the cage on day 10, while in the combination group, one mouse was sacrificed on day 9 due to an ulcer on the tumor. Data are mean ± SEM for $n = 3$–4 mice per group; significant p-values are indicated (one-way ANOVA). Linear regression was used to calculate the correlation coefficient (R^2) and p-value, indicated on each panel in **(D)**.

specific T cells (Fig. 5C). CD8$^+$ T cell rates in the spleen, like in the tumor, were correlated to CD8α^+ cDC1 frequencies; the reduction in M2-like macrophages in combination-treated mice correlated with an increase in CD4$^+$ T cell frequencies and PD-1 expression rates in CD8$^+$ and CD4$^+$CD69$^+$ T cells (Fig. 5D).

DISCUSSION

For patients with melanoma, combined immune checkpoint blockade with nivolumab (anti-PD-1) and ipilimumab (anti-CTLA-4) has improved the 5-year overall survival rate to levels exceeding 50%.[2] Despite this spectacular result, almost half of the patients either fail to respond or develop resistance to treatment. Oncolytic viruses are promising novel therapeutic agents that may help overcome this primary or acquired resistance. They can achieve *in vivo* immunization against cancer, through inducing the release of tumor (neo-)antigens in an immunogenic manner, while transforming the TME into a T cell-inflamed state.[5,7,60] Indeed, Ribas *et al.* clearly demonstrated this principle in patients with advanced melanoma, who received i.t. injections of the oncolytic virus T-VEC (a herpes simplex virus encoding GM-CSF), which, combined with PD-1 blockade, dramatically increased T cell infiltration, not only of injected but also of noninjected lesions.[61]

Myeloid subsets have been recognized as holding the key to ensuring both efficient antitumor T cell priming and attracting effector T cells to the TME. It is therefore vital that oncolytic viruses ensure proper APC development and activation, even in the face of melanoma-associated immune suppression. In our *in vitro* culture model, we found that melanoma cell lines, without exogenously added cytokines, polarized monocytes into CD163$^+$ M2-like macrophages, lacking expression of co-stimulatory markers. Soluble factors implicated in skewing monocytes to M2-like macrophages are M-CSF, IL-6, and IL-10, and are dependent on cross-talk in the TME.[62–65] In our WM9-

based model, M-CSF was the most likely culprit in this context. Of note, macrophages can acquire a composite M1/M2 phenotype on the continuous M1-M2 polarization spectrum[4] in response to various cues in their milieu.[11,22] Although macrophages in WM9 co-cultures did not downregulate CD14 or CD163 upon ORCA-010 infection of the melanoma cells, these macrophages did increase their expression of B7-family ligands (CD80, CD86, and PD-L1), activation markers that are commonly expressed by M1-like macrophages upon interferon- and TLR-mediated signaling.[66] Inflammatory cytokines secreted in the WM9 co-cultures measured on day 8 were not modulated by ORCA-010, which might have been related to consumption of released cytokines in the cultures (Supplementary Fig. S3), and the maintained expression of CD163 on the macrophages could be by continuous M-CSF stimulation in a closed co-culture system,[21,67] or by TLR-mediated activation of monocytes.[67,68]

Eriksson *et al.*[69] demonstrated that CD40L-armed Ad5/35 could lower rates of $CD11b^+CD163^+$ M2-like cells after 5 days of co-culture with human monocytes. However, this was mostly due to the CD40L transgene as, in accordance with our findings, this shift was not observed with the unarmed Ad5/35. It was also the CD40L transgene that induced subsequent IL-12 release by the activated monocyte-derived macrophages. Similarly, in an *in vivo* pancreatic tumor model, the unarmed Ad5/35 oncolytic virus did not impact the M1/M2 ratio, but rather the murine CD40L-expressing virus induced M1-like macrophages.[69] As Ad5-Luc-RGD *per se* could not induce this activation, it is most likely that DAMPs, released upon ORCA-010-induced oncolysis, were responsible. Indeed, Heinio *et al.*[70] demonstrated that infection of SK-MEL28 with an OAdV resulted in the release of DAMPs (such as ATP) that activated moDCs.[26,71] This is in keeping with our own previous observation that oncolysis induced by ORCA-010 was responsible for the activation of melanoma-conditioned moDCs rather than PAMPs derived from the virus itself.[36]

Strikingly, both in melanoma/monocyte co-cultures without differentiation-inducing cytokines presented herein and in co-cultures with DC differentiation-inducing cytokines,[36] the resulting APCs acquired a $CD14^+CD163^+$ M2-like phenotype, which ORCA-010 infection was unable to steer toward M1-like macrophage or $CD1a^+$ moDC differentiation, respectively. However, in both instances, it did induce activation that resulted in an ability of the generated APCs to prime a type-1 T cell response.

In the B16-OVA mouse model, we investigated the immune response to combination therapy of ORCA-010 with PD-1 blockade. ORCA-010, like all OAdV, cannot replicate in murine B16-OVA tumors,[72] but it can infect B16-OVA cells.[73] The resulting antiviral immune response can prime antitumor immunity through epitope spreading, and promote the homing of immune effector cells into tumors through the expression of CCL5 and CXCL10.[74–76] The *in vivo* myeloid-activating effects of ORCA-010 observed in the B16-OVA model may derive from a combination of T cell-induced death of virus-infected tumor cells, leading to the release of activating DAMPs, and direct binding/uptake of the virus, carrying PAMPs, by myeloid cells.[77–79] Both TLR-dependent and TLR-independent signaling are activated in macrophages that phagocytose tumor cell debris and VP.[32] The intracellular sensing of dsDNA of ORCA-010 can also trigger IRF3 and NF-kB transcription factors, activating type-I interferon signaling and proinflammatory cytokine expression (IL-1β and TNF-α).[31,77,80] Consistent with this, i.t. delivery of ORCA-010 facilitated the recruitment of cross-presenting $CD8\alpha^+$ DCs (cDC1 like) and $CD8^+$ T cells to the TME, both known to enable efficacious PD-1 blockade.[51]

Indeed, in concert with PD-1 blockade, $CD69^+CD8^+$ T cell frequencies increased in the tumor. These could potentially develop into tissue-resident memory T cells.[81–83] Functionally, $CD69^+CD8^+$ T cells can secrete IFNγ,[84] induced by the action of anti-PD-1.[74] Likely, as previously described by Spranger *et al.*,[51] recruited cDC1 were responsible for CXCL10 expression, which would subsequently have attracted $CD8^+$ T cells to the TME. This is supported by the observed perfect correlation between frequencies of both subsets in the tumor. Although we did not observe a reduction of M2-like macrophages at the tumor, we showed that M1-like macrophages correlated with PD-1 expression on $CD8^+$ T cells. The failure to demonstrate macrophage modulation by ORCA-010 in the TME may have been due to its inability to induce oncolysis in the mouse model.

Interestingly, we did observe increased M1-like macrophage content in the spleen upon combined ORCA-010 and anti-PD-1 treatment and striking inverse correlations between M2 rates and frequencies of activated $CD8^+$ and $CD4^+$ T cells in the spleen, expressing PD-1, and CD69 and PD-1, respectively. Combination treatment also increased $CD8\alpha^+$ cDC1 rates in the spleen, which correlated with $CD8^+$ T cell frequencies. For now, it remains unclear how i.t. injections of ORCA-010 led to these systemic myeloid subset-modulating effects, but conceivably, adenovirus-induced type-1 IFNs may have been responsible.[85,86]

CONCLUSION

To conclude, ICD of melanoma cells by ORCA-010 activates human macrophages *in vitro*, functionally equipping them to prime and drive a type-1 T cell response. In the B16-OVA melanoma model, i.t. ORCA-010 injection combined with systemic PD-1 blockade mobilized and recruited cDC1 and attracted activated effector T cells to the TME. Interestingly, ORCA-010 and anti-PD-1 combination treatment induced an M2-like macrophage reduction in the spleen, which was accompanied by

increased systemic frequencies of activated $CD4^+$ and $CD8^+$ T cells, expressing PD-1. Altogether, these data clearly support the intratumoral delivery of ORCA-010 to enhance PD-1 blockade efficacy in melanoma.

ACKNOWLEDGMENTS

The authors thank Trang Nguyen, Sinead M. Lougheed, Anita Stam, Dorian Stolk, Riikka Havunen, and the Biomedicum FACS Core Facility (University of Helsinki, Finland) for technical assistance.

AUTHORS' CONTRIBUTIONS

I.M. designed and performed research, analyzed and interpreted data, and wrote the article. M.L.G. performed research, and collected and analyzed data. V.W.v.B. designed research and interpreted data. D.C.A.Q., J.M.S., and V.C.C. provided technical support. W.D. and A.H. provided materials and designed research. R.v.d.V. and T.D.d.G. designed research, analyzed and interpreted data, and wrote the article. All authors read, edited, and approved the article.

AUTHOR DISCLOSURE

I.M. and W.D. have been, or are employed by ORCA Therapeutics. V.W.v.B. serves as CSO for ORCA Therapeutics. J.M.S. is an employee of TILT Biotherapeutics Ltd.. A.H. is shareholder in Targovax ASA and TILT Biotherapeutics Ltd.. T.D.d.G. has served as advisor for TILT Biotherapeutics Ltd.

FUNDING INFORMATION

This study was supported by the European Union's Horizon 2020 Marie Curie research and innovation program (grant agreement no. 643130, VIRION).

SUPPLEMENTARY MATERIAL

Supplementary Figure S1
Supplementary Figure S2
Supplementary Figure S3
Supplementary Table S1
Supplementary Table S2

REFERENCES

1. Morrison C, Pabla S, Conroy JM, et al. Predicting response to checkpoint inhibitors in melanoma beyond PD-L1 and mutational burden. J Immunother Cancer 2018;6:32.
2. Larkin J, Chiarion-Sileni V, Gonzalez R, et al. Five-year survival with combined nivolumab and ipilimumab in advanced melanoma. N Engl J Med 2019;381:1535–1546.
3. Critchley-Thorne RJ, Yan N, Nacu S, et al. Down-regulation of the interferon signaling pathway in T lymphocytes from patients with metastatic melanoma. PLoS Med 2007;4:e176.
4. Chen Y, Song Y, Du W, et al. Tumor-associated macrophages: an accomplice in solid tumor progression. J Biomed Sci 2019;26:78.
5. Blank CU, Haanen JB, Ribas A, et al. Cancer immunology. The "cancer immunogram." Science 2016;352:658–660.
6. Gartrell RD, Marks DK, Hart TD, et al. Quantitative analysis of immune infiltrates in primary melanoma. Cancer Immunol Res 2018;6:481–493.
7. de Graaf JF, de Vor L, Fouchier RAM, et al. Armed oncolytic viruses: a kick-start for anti-tumor immunity. Cytokine Growth Factor Rev 2018;41:28–39.
8. Salmi S, Siiskonen H, Sironen R, et al. The number and localization of CD68+ and CD163+ macrophages in different stages of cutaneous melanoma. Melanoma Res 2019;29:237–247.
9. Franklin RA, Liao W, Sarkar A, et al. The cellular and molecular origin of tumor-associated macrophages. Science 2014;344:921–925.
10. Biswas SK, Mantovani A. Macrophage plasticity and interaction with lymphocyte subsets: cancer as a paradigm. Nat Immunol 2010;11:889–896.
11. Lacey DC, Achuthan A, Fleetwood AJ, et al. Defining GM-CSF- and macrophage-CSF-dependent macrophage responses by in vitro models. J Immunol 2012;188:5752–5765.
12. Kiss M, Van Gassen S, Movahedi K, et al. Myeloid cell heterogeneity in cancer: not a single cell alike. Cell Immunol 2018;330:188–201.
13. Vitale I, Manic G, Coussens LM, et al. Macrophages and metabolism in the tumor microenvironment. Cell Metab 2019;30:36–50.
14. Ruffell B, Coussens LM. Macrophages and therapeutic resistance in cancer. Cancer Cell 2015;27:462–472.
15. Yang L, Zhang Y. Tumor-associated macrophages: from basic research to clinical application. J Hematol Oncol 2017;10:58.
16. Rodriguez RM, Suarez-Alvarez B, Lavin JL, et al. Signal integration and transcriptional regulation of the inflammatory response mediated by the GM-/M-CSF signaling axis in guman monocytes. Cell Rep 2019;29:860–872 e5.
17. Ruffell B, Chang-Strachan D, Chan V, et al. Macrophage IL-10 blocks CD8+ T cell-dependent responses to chemotherapy by suppressing IL-12 expression in intratumoral dendritic cells. Cancer Cell 2014;26:623–637.
18. Loskog A. Immunostimulatory gene therapy using oncolytic viruses as vehicles. Viruses 2015;7:5780–5791.
19. Saio M, Radoja S, Marino M, et al. Tumor-infiltrating macrophages induce apoptosis in activated CD8(+) T cells by a mechanism requiring cell contact and mediated by both the cell-associated form of TNF and nitric oxide. J Immunol 2001;167:5583–5593.
20. Pollard JW. Tumour-educated macrophages promote tumour progression and metastasis. Nat Rev Cancer 2004;4:71–78.
21. Wyckoff J, Wang W, Lin EY, et al. A paracrine loop between tumor cells and macrophages is required for tumor cell migration in mammary tumors. Cancer Res 2004;64:7022–7029.
22. Ambarus CA, Krausz S, van Eijk M, et al. Systematic validation of specific phenotypic markers for in vitro polarized human macrophages. J Immunol Methods 2012;375:196–206.
23. Arnold CE, Gordon P, Barker RN, et al. The activation status of human macrophages presenting antigen determines the efficiency of Th17 responses. Immunobiology 2015;220:10–19.
24. Ylösmäki E, Cerullo V. Design and application of oncolytic viruses for cancer immunotherapy. Curr Opin Biotechnol 2020;65:25–36.

25. Marelli G, Howells A, Lemoine NR, et al. Oncolytic viral therapy and the immune system: a double-edged sword against cancer. Front Immunol 2018; 9:866.

26. Ma J, Ramachandran M, Jin C, et al. Characterization of virus-mediated immunogenic cancer cell death and the consequences for oncolytic virus-based immunotherapy of cancer. Cell Death Dis 2020;11:48.

27. Ferguson TA, Choi J, Green DR. Armed response: how dying cells influence T-cell functions. Immunol Rev 2011;241:77–88.

28. Kaufman HL, Kohlhapp FJ, Zloza A. Oncolytic viruses: a new class of immunotherapy drugs. Nat Rev Drug Discov 2015;14:642–662.

29. Chen CY, Hutzen B, Wedekind MF, et al. Oncolytic virus and PD-1/PD-L1 blockade combination therapy. Oncolytic Virother 2018;7:65–77.

30. Wongthida P, Diaz RM, Galivo F, et al. VSV oncolytic virotherapy in the B16 model depends upon intact MyD88 signaling. Mol Ther 2011;19: 150–158.

31. György F, Freudenberg M, Greber UF, et al. Adenovirus-triggered innate signalling pathways. Eur J Microbiol Immunol 2011;1:279–288.

32. Zhu J, Huang X, Yang Y. Innate immune response to adenoviral vectors is mediated by both Toll-like receptor-dependent and -independent pathways. J Virol 2007;81:3170–3180.

33. Kleijn A, Kloezeman J, E. Treffers-Westerlaken, et al. The therapeutic efficacy of the oncolytic virus Delta24-RGD in a murine glioma model depends primarily on antitumor immunity. Oncoimmunology 2014;3:e955697.

34. Kim JW, Miska J, Young JS, et al. A comparative study of replication-incompetent and -competent adenoviral therapy-mediated immune response in a murine glioma model. Mol Ther 2017;5:97–104.

35. Dong W, J.W. van Ginkel, Au KY, et al. ORCA-010, a novel potency-enhanced oncolytic adenovirus, exerts strong antitumor activity in preclinical models. Hum Gene Ther 2014;25:897–904.

36. Lopez Gonzalez M, van de Ven R, de Haan H, et al. Oncolytic adenovirus ORCA-010 increases the type 1 T cell stimulatory capacity of melanoma-conditioned dendritic cells. Clin Exp Immunol 2020;201:145–160.

37. Herlyn D, Iliopoulos D, Jensen PJ, et al. In vitro properties of human melanoma cells metastatic in nude mice. Cancer Res 1990;50:2296.

38. Van Muijen GNP, Cornelissen LMHA, Jansen CFJ, et al. Antigen expression of metastasizing and non-metastasizing human melanoma cells xenografted into nude mice. Clin Exp Metastasis 1991; 9:259–272.

39. Haluska FG, Tsao H, Wu H, et al. Genetic alterations in signaling pathways in melanoma. Clin Cancer Res 2006;12(7 Pt 2):2301s–2307s.

40. Karasic TB, Hei TK, Ivanov VN. Disruption of IGF-1R signaling increases TRAIL-induced apoptosis: a new potential therapy for the treatment of melanoma. Exp Cell Res 2010;316:1994–2007.

41. Cervera-Carrascon V, Siurala M, Santos JM, et al. TNFa and IL-2 armed adenoviruses enable complete responses by anti-PD-1 checkpoint blockade. Oncoimmunology 2018;7:e1412902.

42. Dmitriev I, Krasnykh V, Miller CR, et al. An adenovirus vector with genetically modified fibers demonstrates expanded tropism via utilization of a coxsackievirus and adenovirus receptor-independent cell entry mechanism. J Virol 1998; 72:9706–9713.

43. Bischoff JR, Kirn DH, Williams A, et al. An adenovirus mutant that replicates selectively in p53-deficient human tumor cells. Science 1996;274: 373–376.

44. Suzuki K, Fueyo J, Krasnykh V, et al. A conditionally replicative adenovirus with enhanced infectivity shows improved oncolytic potency. Clin Cancer Res 2001;7:120–126.

45. Chen H, Schurch CM, Noble K, et al. Functional comparison of PBMCs isolated by Cell Preparation Tubes (CPT) vs. Lymphoprep Tubes. BMC Immunol 2020;21:15.

46. Li G, Hangoc G, Broxmeyer HE. Interleukin-10 in combination with M-CSF and IL-4 contributes to development of the rare population of CD14+CD16++ cells derived from human monocytes. Biochem Biophys Res Commun 2004;322: 637–643.

47. Puig-Kroger A, Sierra-Filardi E, Dominguez-Soto A, et al. Folate receptor beta is expressed by tumor-associated macrophages and constitutes a marker for M2 anti-inflammatory/regulatory macrophages. Cancer Res 2009;69:9395–9403.

48. Leon B, Martinez del Hoyo G, Parrillas V, et al. Dendritic cell differentiation potential of mouse monocytes: monocytes represent immediate precursors of CD8- and CD8+ splenic dendritic cells. Blood 2004;103:2668–2676.

49. Stoitzner P, Green LK, Jung JY, et al. Inefficient presentation of tumor-derived antigen by tumor-infiltrating dendritic cells. Cancer Immunol Immunother 2008;57:1665–1673.

50. Wang B, Li Q, Qin L, et al. Transition of tumor-associated macrophages from MHC class IIhi to MHC class IIlow mediates tumor progression in mice. BMC Immunol 2011;12:43.

51. Spranger S, Bao R, Gajewski TF. Melanoma-intrinsic beta-catenin signalling prevents anti-tumour immunity. Nature 2015;523:231–235.

52. van Hooren L, Georganaki M, Huang H, et al. Sunitinib enhances the antitumor responses of agonistic CD40-antibody by reducing MDSCs and synergistically improving endothelial activation and T-cell recruitment. Oncotarget 2016;7:50277–50289.

53. Arlauckas SP, Garris CS, Kohler RH, et al. In vivo imaging reveals a tumor-associated macrophage-mediated resistance pathway in anti-PD-1 therapy. Sci Transl Med 2017;9:eaal3604 .

54. Botelho NK, Tschumi BO, Hubbell JA, et al. Combination of synthetic long peptides and XCL1 fusion proteins results in superior tumor control. Front Immunol 2019;10:294.

55. Di Martile M, Farini V, Consonni FM, et al. Melanoma-specific bcl-2 promotes a protumoral M2-like phenotype by tumor-associated macrophages. J Immunother Cancer 2020;8:e000489.

56. van Dinther D, Veninga H, Iborra S, et al. Functional CD169 on macrophages mediates interaction with dendritic cells for CD8(+) T cell cross-priming. Cell Rep 2018;22:1484–1495.

57. Peng WY, Chen JQ, Liu CW, et al. Loss of PTEN promotes resistance to T cell-mediated immunotherapy. Cancer Res 2016;6:202–216.

58. Gros A, Robbins PF, Yao X, et al. PD-1 identifies the patient-specific CD8(+) tumor-reactive repertoire infiltrating human tumors. J Clin Invest 2014; 124:2246–2259.

59. Fernandez-Poma SM, Salas-Benito D, Lozano T, et al. Expansion of tumor-infiltrating CD8(+) T cells expressing PD-1 improves the efficacy of adoptive T-cell therapy. Cancer Res 2017;77: 3672–3684.

60. Duan Q, Zhang H, Zheng J, et al. Turning cold into hot: firing up the tumor microenvironment. Trends Cancer 2020;6:605–618.

61. Ribas A, Dummer R, Puzanov I, et al. Oncolytic virotherapy promotes intratumoral T cell infiltration and improves anti-PD-1 immunotherapy. Cell 2017;170:1109–1119 e10.

62. Chomarat P, Banchereau J, Davoust J, et al. IL-6 switches the differentiation of monocytes from dendritic cells to macrophages. Nat Immunol 2000;1:510–514.

63. Heusinkveld M, van Steenwijk PJD, Goedemans R, et al. M2 Macrophages induced by prostaglandin E2 and IL-6 from cervical carcinoma are switched to activated M1 macrophages by CD4(+) Th1 cells. J Immunol 2011;187:1157–1165.

64. Lindenberg JJ, van de Ven R, Lougheed SM, et al. Functional characterization of a STAT3-dependent dendritic cell-derived CD14(+) cell population arising upon IL-10-driven maturation. Oncoimmunology 2013;2:e23837.

65. Michielon E, López González M, Burm JL, et al. Micro-environmental cross-talk in an organotypic human melanoma-in-skin model directs M2-like monocyte differentiation via IL-10. Cancer Immunol Immunother 2020;69:1–13.

66. Wang N, Liang HW, Zen K. Molecular mechanisms that influence the macrophage M1-M2 polarization balance. Front Immunol 2014;5:614.

67. Buechler C, Ritter M, Orso E, et al. Regulation of scavenger receptor CD163 expression in human monocytes and macrophages by pro- and antiinflammatory stimuli. J Leukocyte Biol 2000;67:97–103.

68. Weaver LK, Pioli PA, Wardwell K, et al. Up-regulation of human monocyte CD163 upon activation of cell-surface Toll-like receptors. J Leukocyte Biol 2007;81:663–671.

69. Eriksson E, Moreno R, Milenova I, et al. Activation of myeloid and endothelial cells by CD40L gene therapy supports T-cell expansion and migration into the tumor microenvironment. Gene Ther 2017; 24:92–103.

70. Heinio C, Havunen R, Siurala M, et al. Molecular insight into pathogen-associated molecular pattern signaling during TNFa and IL2 armed oncolytic adenovirus treatments. Cancer Immunol Res 2020;8:53–54.

71. Venereau E, Ceriotti C, Bianchi ME. DAMPs from cell death to new life. Front Immunol 2015;6:422.

72. Santos JM, Havunen R, Siurala M, et al. Adenoviral production of interleukin-2 at the tumor site removes the need for systemic postconditioning in adoptive cell therapy. Int J Cancer 2017;141: 1458–1468.

73. Okada Y, Okada N, Nakagawa S, et al. Tumor necrosis factor alpha-gene therapy for an established murine melanoma using RGD (Arg-Gly-Asp) fiber-mutant adenovirus vectors. Jpn J Cancer Res 2002;93:436–444.

74. Peng W, Liu C, Xu C, et al. PD-1 blockade enhances T-cell migration to tumors by elevating IFN-gamma inducible chemokines. Cancer Res 2012;72:5209–5218.

75. Gujar S, Pol JG, Kim Y, et al. Antitumor benefits of antiviral immunity: an underappreciated aspect of oncolytic virotherapies. Trends Immunol 2018;39: 209–221.

76. Trujillo JA, Sweis RF, Bao R, et al. T cell-inflamed versus non-T cell-inflamed tumors: a conceptual framework for cancer immunotherapy drug development and combination therapy selection. Cancer Immunol Res 2018;6:990–1000.

77. Nociari M, Ocheretina O, Schoggins JW, et al. Sensing infection by adenovirus: toll-like receptor-independent viral DNA recognition signals activation of the interferon regulatory factor 3 master regulator. J Virol 2007;81:4145–4157.

78. Kanerva A, Nokisalmi P, Diaconu I, et al. Antiviral and antitumor T-cell immunity in patients treated with GM-CSF-coding oncolytic adenovirus. Clin Cancer Res 2013;19:2734–2744.

79. Woller N, Gurlevik E, Fleischmann-Mundt B, et al. Viral infection of tumors overcomes resistance to PD-1-immunotherapy by broadening neoantigenome-directed T-cell responses. Mol Ther 2015;23:1630–1640.

80. Shaw AR, Suzuki M. Immunology of adenoviral vectors in cancer therapy. Mol Ther 2019;15:418–429.

81. Sancho D, Gomez M, Sanchez-Madrid F. CD69 is an immunoregulatory molecule induced following activation. Trends Immunol 2005;26: 136–140.

82. Mackay LK, Braun A, Macleod BL, et al. Cutting edge: CD69 interference with sphingosine-1-phosphate receptor function regulates peripheral T cell retention. J Immunol 2015;194:2059–2063.

83. Osborn JF, Hobbs SJ, Mooster JL, et al. Central memory CD8+ T cells become CD69+ tissue-residents during viral skin infection independent of CD62L-mediated lymph node surveillance. PLoS Pathog 2019;15:e1007633.

84. Sucker A, Zhao F, Pieper N, et al. Acquired IFN-gamma resistance impairs anti-tumor immunity and gives rise to T-cell-resistant melanoma lesions. Nat Commun 2017;8:15440.

85. Huarte E, Larrea E, Hernández-Alcoceba R, et al. Recombinant adenoviral vectors turn on the type I interferon system without inhibition of transgene expression and viral replication. Mol Ther 2006; 14:129–138.

86. Minamitani T, Iwakiri D, Takada K. Adenovirus virus-associated RNAs induce type I interferon expression through a RIG-I-mediated pathway. J Virol 2011;85:4035–4040.

Received for publication October 14, 2020;
accepted after revision January 14, 2021.

Published online: January 19, 2021.